This is a previous version of the article published by Elsevier in Electrochimica Acta. 2011, 58: 184-192. doi:10.1016/j.electacta.2011.09.029

On the behavior of the Pt(100) and vicinal surfaces in alkaline media.

Rosa M. Aran-Ais, Marta C. Figueiredo, Francisco J. Vidal-Iglesias, Victor Climent, Enrique Herrero[*], *Juan M. Feliu*

Instituto de Electroquímica, Universidad de Alicante, Apt 99, E-03080, Alicante, Spain

Abstract:

We address in this paper a voltammetric study of the charge transfer processes characteristic of Pt(100) and vicinal surfaces in alkaline media. The electrochemical behavior of a series of stepped surfaces of the type Pt(S)[n(100)×(111)] has been characterized using cyclic voltammetry at different pHs, charge displacement measurements and FTIR experiments for adsorbed CO. The results from these techniques allow assigning the different peaks appearing in the voltammogram to hydrogen and /or OH adsorption on the different sites characteristic of these surfaces, namely, terrace and step sites. Additionally, the potential of zero total charge (pztc) of the electrodes was also determined. The resulting pztc values shift to more negative values when the step density increases on the surface up to n=5. FTIR spectroscopy experiments have been used to monitor the adsorption of CO on the different surfaces as well as the consequent CO oxidation, accompanying a positive potential sweep. The oxidation of adsorbed CO on (100) terraces is catalyzed by the presence of the (111) steps. The FTIR spectra revealed that CO is mostly bonded in bridge configuration at low potentials interconverting to on-top when the electrode potential is increased.

---

[*] Corresponding Author

e-mail address: herrero@ua.es

Fax.: +34965903537

Keywords: Pt(100) stepped surfaces, NaOH, pztc, CO charge displacement, CO oxidation

1. Introduction:

Well-defined platinum surfaces are important tools for the understanding of the electrochemical reactivity of catalytic reactions at a molecular level. The structure and composition of the surface are parameters with great influence on its reactivity [1]. Among basal planes, the behavior of the Pt(100) electrode is still not completely understood. The voltammetric profile of the Pt(100) electrode is extremely sensitive to the preparation and pre-treatment conditions [2]. In acidic media, two extreme voltammetric profiles can be obtained after flame annealing, depending on the cooling conditions [3]. The first one, obtained after cooling the electrode in air, corresponds to a clean but two-dimensionally disordered surface. In order to obtain two-dimensionally ordered Pt(100) terraces, reductive cooling conditions, i.e. avoiding oxygen adsorption, have to be used [4]. Additional experiments [5-7] showed that the treatment of the Pt(100) electrode under reductive cooling conditions leads to an electrode with wide ordered terraces. Such delicate sensitivity of the surface structure to the treatment conditions is probably the main reason for the difficulty in understanding the charge transfer processes involved in the voltammetric response from stepped surfaces vicinal to the (100) pole. These surfaces were characterized from the point of view of electric charge density measurements, in acidic media [8-10]. The reported results revealed that the hydrogen coverage on terraces appears to be slightly lower than that corresponding to one electron per terrace site while the charge measured in the lower potential range (below 0.2V, assigned to hydrogen adsorption on (111) defects) was larger than that expected for well-ordered surfaces [8].

In alkaline media, the number of studies for the Pt(100) electrode is rather scarce [11-16]. Additionally, there is not a general agreement on the correct voltammetric profile for the ordered Pt(100) electrode. In general, four peaks can be observed, but their relative magnitude depends on the cooling conditions, the supporting electrolyte and the quality of the crystal.

For this reason, it seems important to systematically analyze the influence of the surface order in the origin of the different voltammetric features. The best way to study this effect is the use of surfaces with controlled amount of defects, such as these on stepped surface electrodes, and to take advantage of the charge displacement experiments to separate different contributions from the voltammograms according to the sign of the associated total charge [17]. Additionally, the extrapolation of the behavior of the stepped surfaces has been used to obtain the expected behavior of the ideal "defect-free" surface [8, 18].

In this work, the voltammetric profile and charge density values determined from stepped surfaces of the type Pt(S)[n(100)×(111)] will be analyzed in alkaline media. The aim is to report the voltammetric characteristics of these surfaces as well as the determination of the different species involved in the charge transfer. Values of the potential of zero total charge (pztc) deduced from CO charge displacement experiments will be related to the step density. Fourier transform infrared (FTIR) spectroscopy experiments have been used to monitor the adsorption of CO on the different surfaces as well as the consequent CO oxidation.

2. Experimental.

Platinum single crystal stepped surfaces were used as working electrodes. They were made by fusion and subsequent slow crystallization of a 99,999% platinum wire, which after careful cooling, were cut and polished following the procedure described in reference [19]. Stepped electrodes used in this work were those vicinal to the (100) pole, in the crystallographic [011] zone. These surfaces have Miller indices Pt(2n-1, 1, 1), where n denotes the number of atom rows on the (100) terraces separated by monoatomic (111) steps. Therefore, these surfaces can also be represented as Pt(S)[n(100)×(111)] in the terrace-step notation proposed by Lang et al. [20]. The number of terrace atoms for the surfaces studied

are n = 20, 15, 12, 8, 6, 4, 3 and 2. This latter surface, Pt(311), represents the turning point in the crystallographic [011] zone, and can be alternatively noted as Pt(S)[2(111)×(100)], that belongs to the Pt(S)[n(111)×(100)] series whose Miller indices are Pt(n+1, n-1, n-1). The step density of these electrodes is defined by the following equation:

$$N_{(100)\times(111)} = \frac{1}{d\left(n-\frac{1}{2}\right)} \quad (1)$$

where *d* is the atomic diameter of platinum (0.278 nm)

Before each experiment, the single crystal electrodes were flame-annealed, cooled down in a reductive atmosphere (H_2+Ar) and quenched with ultra-pure water. It is well known that this treatment leads to surface topographies reasonably close to the nominal ones [9, 21]. Experiments were performed at room temperature in a three electrode electrochemical cell de-aerated by using argon (Air Liquide, N50). The counter electrode was a platinum wire and the potentials were measured against a reversible hydrogen (Air Liquide, N50) electrode (RHE) connected to the cell through a Luggin capillary. Working electrodes have been characterized by cyclic voltammetry in a solution made of 0.1 M NaOH, pH ca. 13 (Merck Suprapur, 99.999%) and ultrapure water from Elga, 18.2 MΩ cm. For the lower pH (7 and 9) phosphate buffer solution was prepared with the appropriate amounts of sodium dihydrogen phosphate and disodium hydrogen phosphate (Merck Suprapur). The electrode potential was controlled using an EG&G PARC 175 signal generator in combination with an eDAQ EA161 potentiostat and currents where recorded using an eDAQ e-corder ED401 recording system.

The experimental set-up for CO (Air Liquide, N47) charge displacement studies has been described in references [22-24]. Prior to CO adsorption, the voltammogram of the oriented platinum electrodes in the test electrolyte was recorded. The potential was held constant at 0.1 V while a stream of CO flew into the cell, and the current-time transient was

recorded until the transient current was steadily zero. After saturation of the platinum surface by adsorbed CO, the excess CO was eliminated from the solution and cell atmosphere by flowing argon for 15 min, while keeping the electrode potential under control. Then, three voltammograms were recorded: (i) for the control of full surface blocking, in the lower potential range (0.06-0. 4 V); (ii) for the electrochemical stripping and measurement of the amount of adsorbed CO; (iii) for monitoring the recovery of hydrogen adsorption capability of the CO-free surface.

Spectroelectrochemical experiments were performed with a Nicolet Magna 850 spectrometer equipped with a MCT detector. The spectroelectrochemical cell was provided with a prismatic CaF_2 window beveled at 60º. Spectra shown are composed of 200 interferograms collected with a resolution of 8 cm^{-1} and p polarized light. They are presented as absorbance, according to $A= - \log (R/R_0)$ where R and R_0 are the reflectance corresponding to the single beam spectra obtained at the sample and reference potentials, respectively. All the spectroelectrochemical experiments were also performed at room temperature, with a reversible hydrogen electrode (RHE) and a platinum wire used as reference and counter electrodes, respectively.

3. Results and discussion.

3.1. Cyclic Voltammetry

The voltammetric profiles measured for Pt (S) [n(100)×(111)] surfaces in 0.1 M NaOH are presented in figure 1. As can be seen, the profile corresponding to the Pt(100) surface shows four reversible peaks at 0.290, 0.395, 0.465 and 0.570 V vs. RHE. These results are in agreement with previous reports in the literature [11, 14-16]. When compared to the profile obtained in acid media (figure 2), significant differences can be observed. In absence of specific adsorption, two main broad features can be distinguished in acid media

centered at approximately, 0.40 and 0.55 V and are assigned to the adsorption of hydrogen and OH on the terraces, respectively. [8, 25]. The small peak at 0.30 V has been assigned to hydrogen adsorption on terrace edges as deduced from the evolution of this peak after the deliberate introduction of steps on the surface [8]. The presence of four different contributions in alkaline media indicates that the adsorption processes of hydrogen and OH in alkaline media are more complex. Additionally, some of the states corresponding to the adsorption of hydrogen or/and OH have been displaced to more positive potentials. However, the measured charge between 0.2 and 0.7 V without any double layer correction is 323 μC cm^{-2}, very similar to that measured in acid (303 μC cm^{-2} [8]) which suggests that the hydrogen and OH coverages are very similar. Another remarkable difference between the voltammetric responses recorded in both media is related to the adsorption processes below 0.2 V. In the case of the alkaline media, the current measured in this potential range features a shape typically assigned to double layer contributions whereas in acid media, some adsorption processes are clearly visible.

The addition of (111) steps to the surface induces significant changes on the CV profiles, especially on the peaks at 0.395 and 0.465 V. The behavior of the (100) vicinal surfaces can be divided in two different groups, the surfaces with wide terraces ($n \geq 7$) and the surfaces with narrow terraces. For the surfaces with wide terraces, the changes are small. The peak at 0.465 V decreases and shifts towards higher potential values when the step density increases. From this behavior, it is clear that this peak is associated to adsorption processes on terrace sites. On the other hand, the current density for the peak at 0.395 V increases and the peak potential shifts to higher values. It should be mentioned that this signal for the Pt(100) electrode is just a very small peak superimposed to a broad feature. The broad feature remains almost constant with the step density for surfaces with wide terraces and the peak at 0.395 V increases. Thus, the small peak that develops as the step density increases can be assigned to a

response from species adsorbed on step sites. The other two peaks, those at 0.290 and 0.570 V, are not significantly affected by the increasing presence of steps on the surface for n>7; in fact, the peak shape and current is almost not affected by the step density. Also at potentials lower than 0.2 V changes after introduction of steps are very small.

For the surfaces with narrow terraces (Figure 1, bottom panel) changes in the voltammogram are dramatic. The contributions above 0.46 V previously discussed completely disappear and the one at 0.395 V associated to the presence of step sites becomes the predominant feature of the voltammogram. This peak becomes broader and shifts to higher potentials. Additionally, the introduction of steps causes similar effects as those observed in acidic media for the potentials below 0.2V, [8]. The current of this region increases as the step density increases.

Since the differences between acid and basic media are significant, it is important to study intermediate pH values. Concomitantly, information is obtained about the effect of adsorbing anions. The voltammograms of the stepped surfaces on the (100) pole at pH 9 and 7 in phosphate buffered solutions are presented in figure 3. In panel C, the voltammograms of the Pt(100) electrode at three different pH's are compared. As can be seen, the major differences are located in the region above 0.4 V, whereas the voltammetric profile remains almost constant below that potential. Additionally, the peaks at 0.465 and 0.570 V shift in opposite directions. The peak at 0.570 V shifts towards higher potential values when the pH is decreased and eventually disappears at pH 7, whereas that at 0.465 V moves in the opposite direction and its charge increases. From the shifts described above and the comparison with the behavior observed for the Pt(100) electrode when sulfate anions are added to perchloric acid solutions [26], it can be proposed that the peak at 0.465 V corresponds to the competitive adsorption of hydrogen/anions and the peak at 0.570 V corresponds to the adsorption of OH. It should be stressed that the reference electrode used in this work (RHE) is sensitive to the

proton concentration and, therefore, the shifts just described are different from the simple nernstian displacement of the adsorption potential and reflect the competitive behavior between hydrogen / OH and anions. Finally, it is also interesting to note that the two peaks at 0.395 and 0.29 V, visible in the voltammogram recorded in 0.1 M NaOH, merge into one single peak at 0.3 V when pH is decreased to 7. An intermediate situation is observed at pH 9.

For the stepped surfaces, the changes upon increasing the step density are similar to those observed in 0.1 M NaOH. In all the cases, the current at potentials below 0.2 V increases with the steps density of the surface, revealing that independently from the pH, hydrogen adsorption on the steps occurs in this potential window, as has been also proposed for acid media [27]. At pH 7, fewer peaks are observed in the CV probably as a consequence of the adsorption of phosphate anions. Regarding the pH dependence of peak potentials, for those processes associated with terrace sites (those at 0.465 and 0.570 V), the evolution is equivalent to that observed to the Pt(100) electrode. Figure 4 shows the variation of peak potentials with the pH of the solution for the Pt(15,1,1) surface. The peaks at 0.32-0.39 V and 0.42-0.47 V move less that 60mV per pH unit in the SHE scale (around 50 mV). Since anion adsorption is expected to be pH independent in the SHE scale at pH values in which the acid is completely dissociated (i.e., shift 59 mV per pH unit in a RHE scale) and hydrogen adsorption should shift 59 mV per pH unit (i.e., should be pH independent in the RHE scale), we conclude that hydrogen as well as anion competitive adsorption are involved in those peaks, since intermediate shifts are observed. On the other hand, the peak at 0.295 V does not change its potential in the RHE scale, that is, the peak shifts 59 mV per pH unity in the SHE scale. Thus, it can be suggested that this process is related only to hydrogen adsorption. It should be noted that the changes in this region between acid and basic media are very small (there is only a slight shift in the signals), which also suggest that the process is mainly related to hydrogen adsorption.

As a summary, it can be said that the processes below 0.3 V correspond to the adsorption of hydrogen, whereas those occurring above 0.55 V correspond to the adsorption of OH at pH=13. In the region between both values, the adsorption of hydrogen and anions contribute to shape the different peaks in the voltammogram.

3.2. Charge displacement measurements

The careful analysis of the voltammetric profiles obtained for Pt single crystals in alkaline media reveals that the processes that appear between 0.3 and 0.5 V do not correspond to a single charge transfer process. At least two pseudo-capacitive double layer processes can be considered to occur in addition to purely capacitive double layer contributions. These contributions are related to hydrogen adsorption/anion desorption and to hydrogen desorption/ anion adsorption contributions, which take place in the negative and positive-going sweeps, respectively. In pH=13, the anion present in solution is the OH^- species. To discriminate between these two main pseudo-capacitive processes, CO displacement experiments were performed. The experiments of charge displacement were carried out by adsorption of gaseous CO, dosed in the cell atmosphere at 0.1 V. The experimental values of the displaced charges correspond to oxidation processes, as expected in all experiments performed at low displacement potential values [28]. These charges would correspond to oxidative displacement of adsorbed hydrogen following the overall reaction:

$$Pt-H + CO \rightarrow Pt-CO + H^+ + e^- \quad (2)$$

The displaced charge densities obtained are plotted in Fig. 5 versus 1/(n-1/2), which is proportional to the step density (see equation (1)). It can be seen that the plots of displaced charges are linear versus the step density for n>4, following the relationship:

$$q^{0.1\,\mathrm{V}} / \mu\mathrm{C\ cm^{-2}} = -222 + \frac{219}{n - \frac{1}{2}} \qquad (3)$$

As usual, the surfaces with very narrow terraces deviate from the expected behavior. In these cases, the contributions of the steps and terraces to the behavior of the surface cannot be considered independent, since the electronic perturbation created by the step reaches the whole terrace and interacts with the next step.

As has been summarized elsewhere [29], the comparison of displaced charge values and the charges measured from the voltammetric profiles enables the possibility of plotting charge density - potential curves. This points out that both charge measurements are consistent in different experiments, as was shown earlier with other electrode surfaces [30]. The determination of the charge in this combined approach uses the equation:

$$q_E = \int_{E^*}^{E} \frac{|\,j\,|}{\nu} - q_{dis,E^*} \qquad (4)$$

where q_E is the total charge at the applied potential E, j is the voltammetric current density, v is the scan rate and $q_{dis,\,E^*}$ is the charge displaced at the potential E* (in the present case E* is 0.10 V), which is equal but with opposite sign to the charge present on the electrode at this potential. This approach neglects the residual free charge that remains on the CO covered electrode, which has been shown to be very small [31, 32].

The resulting curves have been plotted in figure 6. As usual, the electrode charge densities increase with potential, because the amount of adsorbed hydrogen decreases, and cross the potential axis at a value that would correspond to zero displaced charge. This latter value may be identified with the pztc within the validity of the above approximations [33].

With the charge curves it is now possible to examine how the step density affects the total charge of the electrode at different potential values. One important point is 0.20 V, since

this potential value is always located in an apparent double layer region for all the surfaces studied, since the measured current densities are the same as those at 0.75 V. These charge values are plotted in figure 5. As in the previous case, a linear relationship is obtained for n>4. The equation of the fitting is:

$$q^{0.2\,\mathrm{V}} \;/\,\mu\mathrm{C\ cm^{-2}} = -213 + \frac{294}{n-\frac{1}{2}} \tag{5}$$

This result needs to be explained by considering the hard sphere model for the surfaces studied. For the surfaces in this zone, the area of the unit cell is:

$$A = d^2\left(n-\frac{1}{2}\right) \tag{6}$$

where d is the atomic diameter of platinum. Accordingly, the charge corresponding to one electron process for each unit cell is

$$q_{1e/u.c.} = \frac{e}{A} = \frac{e}{d^2}\left(n-\frac{1}{2}\right)^{-1} = \frac{q_{100}}{\left(n-\frac{1}{2}\right)} \tag{7}$$

where q_{100} = 209 μC cm^{-2} is the charge corresponding to one electron per platinum atom on the (1×1)(100) surface. The unit cell contains n rows of atoms, n-1 pertaining to the terrace and one corresponding to the step. The charge corresponding to a one electron process affecting only the n-1 rows of atoms on the terrace would be:

$$q_{n-1} = (n-1)\,q_{1e/u.c.} = q_{100}\,\frac{n-1}{n-\frac{1}{2}} = q_{100} - \frac{1}{2}q_{100}\,\frac{1}{n-\frac{1}{2}} \tag{8}$$

In this case, the plot of the charge as a function of 1/(n-1/2) would give a slope of ca. 105 μC cm^{-2}. Such slope was observed with the total charges measured in acid media at 0.2 V [8], implying that, under such conditions, (n-1) atoms from the terraces are covered with hydrogen. Conversely, the results shown in figure 5, measured in alkaline solution, exhibit an

slope that is nearly double than that predicted in equation (8). To explain this result, we could consider that only *n*-2 atoms are covered by hydrogen. In this case, the following relationship is obtained:

$$q_{n-2} = (n-2)\,q_{1e/u.c.} = q_{100}\frac{n-2}{n-\frac{1}{2}} = q_{100} - \frac{3}{2}q_{100}\frac{1}{n-\frac{1}{2}} \qquad (9)$$

Although this equation predicts very well the experimental slope observed in figure 5, the fact that one row of platinum atoms remains uncovered by hydrogen at this potential is quite unexpected. The most straightforward explanation for this result would be that the row closer to the step sites is blocked by the anion (in this case, OH) adsorbed on these sites. However, the charge of these anions would also contribute to the total charge. For instance, if we consider one OH per step atom, the total charge would be:

$$q_{total} = -q_H + q_{OH} = -(n-2)\,q_{1e/u.c.} + q_{1e/u.c.} = (n-3)\,q_{1e/u.c.} = q_{100} - \frac{5}{2}q_{100}\frac{1}{n-\frac{1}{2}} \qquad (10)$$

and the resulting slope would be now much higher than the observed one. According to the previous arguments, the best explanation for the observed slope is to consider that the OH coverage on step sites is one half, blocking only one half of the atoms adjacent to the step site:

$$q_{total} = -q_H + q_{OH} = -\left(n-1-\frac{1}{2}\right)q_{1e/u.c.} + \frac{1}{2}q_{1e/u.c.} = (n-2)\,q_{1e/u.c.} = q_{100} - \frac{3}{2}q_{100}\frac{1}{n-\frac{1}{2}}$$

The intercept and slope obtained here are, within the experimental error, the same as those obtained in acid solutions containing bromide at 0.150 V [9]. In that case, it was proposed that two different species were adsorbed on the surface: 1) bromide atoms were adsorbed on the step with a coverage of 0.5 and these atoms were blocking half a terrace row and 2) in the remaining terrace sites the hydrogen coverage was 1. A similar situation can be proposed here, just simply by replacing the bromide atoms by adsorbed OH. This means that at 0.20 V

the steps are covered with OH with a coverage value of 0.5, and these species block some terrace sites and hydrogen is adsorbed on the terrace with a ratio of 1 atom per non-blocked platinum terrace site. The situation in which the adsorbed anion on the step blocks some sites on the terrace has been observed not only for bromide but also for acetate. When the solution contains acetate, the peak at 0.26 V is linked to the desorption/adsorption of acetate on the steps and the adsorption of hydrogen on the terrace sites previously blocked by acetate [8].

It should be highlighted that the charge for the Pt(100) electrode deviates from the expected value, that is, the measured charge is ca. 20 μC cm^{-2} lower than that obtained from the extrapolation from the vicinal surfaces with wide terraces. In fact, the measured charge is comparable to that obtained with the Pt(23,1,1) electrode. In UHV environments, Pt(100) electrodes are known to form a reconstructed hexagonal surface structure upon thermal treatment and the reconstruction is lifted when the electrode is put in contact with the solution or during the cooling in the hydrogen/argon atmosphere [7]. In the hexagonal structure, the platinum atoms are about 24% more densely packed than in the unreconstructed surface and when the reconstruction is lifted, the excess of atoms forms islands. In surfaces with wide terraces, the reconstruction process does not take place [8]. For that reason, the Pt(100) electrode can have a higher defect density than the step density of the surfaces with wide terraces for which the reconstruction does not take place. This fact can justify that the level of defects on the Pt(100) surface is similar to the Pt(23,1,1) surface. In fact, the presence of additional defects on the surface of the Pt(100) electrode has been also proposed when the behavior of the Pt(100) electrode is compared with that of the stepped surfaces for structure sensitive reactions, such as methanol and formic acid oxidation [34-36].

Another important potential value to determine the charge density is 0.70 V, where it is expected that only OH is adsorbed on the surface. The total charge values are plotted also in figure 5 as a function of the step density. As can be seen the charge for the surfaces with wide

terraces is ca. 130 μC cm^{-2}. This charge is compatible with a process transferring 1 electron per 2 sites on the terrace. Two different processes can give such value: either the surface at 0.7 V has an OH coverage of 0.5 or the adsorbed species is atomic oxygen with a coverage value of 0.25. Owing to the reversibility of the voltammetric profile, the proposed species is adsorbed OH, since oxygen adsorption is normally an irreversible process [37, 38]. Additionally, the comparison between the charge curves for the Pt(100) in acid and alkaline media (figure 2) indicates that the situation at 0.1 and 0.7 V for both surfaces is almost identical, since the total charge is very similar. However, the change in pH leads to different voltammograms, that is, the pH affects the development of the process. Since the surface is the same, these changes have to be related to the different energies of the hydrated H^+ and OH^- in the bulk water and also the interactions of adsorbed hydrogen and OH with the water molecules as the pH changes. Thus, it is clear that the properties of water affect the adsorption energy, and small changes in this energy can lead to significant changes in the voltammogram, as has been proposed for OH adsorption on the Pt(111) [37].

From the total charge curves in figure 6, the potential of zero total charge (E_{pztc}) can be determined. The values of the E_{pztc} vs. 1/(n-½) are plotted in figure 7. Two different regions can be observed in this plot. For surfaces with n≥8, the changes of the pztc are very small: from the Pt(100) to the Pt(15,1,1) the change is ca. 10 mV. From that point, the values diminish significantly. This dual behavior also corresponds to the observed changes in the voltammetry, since the surfaces having n<8 show a dramatic change in the voltammogram with respect to the others. In order to understand these differences, the charge curves have been plotted in the same graph with the voltammogram (figure 8).

First of all, the nature of all the processes taking place at the surface has to be understood. From the charge analysis it is clear that at 0.10 V, the only species on the surfaces with n>4 is adsorbed hydrogen on the terrace sites and OH on the step sites, whereas at 0.70

V, the OH is adsorbed both on the terrace and step sites. Thus, the signals that increase with the step density should be associated to OH adsorbed on the step sites. Thus, the peak at 0.395 V should correspond to OH adsorbed on the terrace sites. On the other hand, the signals at 0.295, 0.465 and 0.570 V should correspond to processes associated to terraces, since they diminish as the step density increases. From the position of the pztc and the effect of the specific adsorption of phosphate anions and the shift with the pH, it is clear that the process at 0.295 V should correspond to hydrogen adsorbed on the terrace and the peak at 0.570 V is related to OH adsorption on the terrace.

For the process at 0.465 V, since it is very close to the pztc a mixed situation is found. The pztc defines the point where the total charge is zero, that is, the charge contribution of the adsorbed species on the surface counterbalances and gives a zero result (always assuming that the contributions of the diffuse layer are very small). In the present case, this means that the coverage of adsorbed hydrogen and OH are equal, but not individually equal to zero. In the only case where the coverage can be assumed as zero is when the pztc of a given surface lies in a double layer region. In this case, since the current measured in the pztc for the Pt(100) is large, the coverages for both species can be significant. Thus, the peak at 0.495 is mainly associated to OH adsorption on the terrace sites with a significant contribution also from H adsorption on the same sites.

For the surfaces with $n \leq 4$, the situation is not as clear as for the other surfaces since they deviate from the predicted behavior. Probably the peak at 0.39 V involves the competitive adsorption process of OH and H on both terrace and step sites, since the pztc lies in the peak region.

Once the signals have been assigned to the different processes, the changes in the pztc can be understood. From the Pt(100) to the Pt(23,1,1), a new process linked to the adsorption of OH appears at 0.395 V. Since this potential is lower than the pztc, the pztc should move to

more negative potential values. However, since the currents at the pztc are large, the additional charge transferred for the OH adsorption can be easily compensated with a small change in the pztc. Only when the current in this value has diminished significantly, that is for the Pt(11,1,1) electrode, does the pztc diminish from the value measured for the Pt(100). A similar situation was found for these surfaces in acid media in the presence of bromide [9], where the changes in the pztc where buffered by the large current measured in this potential region.

3.3. CO oxidation

As a final step of the displacement experiments, the oxidation of the resulting CO adlayer was carried out in order to assess that the initial state of the electrode can be recovered. In these experiments the dosing of CO is carried out under mild conditions, i.e. the main objective is just to obtain a fully blocked surface. This situation is not necessarily equivalent to that corresponding to the maximum saturation CO coverage that will require the use of saturated CO solutions. It is well known that the CO oxidation kinetics depends strongly on the CO coverage [39-41] and that the potential of the CO stripping peak changes significantly with this parameter. Despite this statement, rough conclusions can be attained about the influence of the steps on the oxidation of CO. In this way, Figure 9 shows the different stripping peaks obtained for the surfaces. As can be seen, the steps catalyze the oxidation of CO for $n \geq 6$ as deduced from the negative shift of the peak potential. In fact, the behavior is qualitatively identical to that observed for this reaction in acid media [8].

When this behavior is compared to that observed for other stepped surfaces in alkaline media, a significant difference appears. For the surfaces vicinal to the Pt(111) electrode, stripping voltammetry for CO shows peaks corresponding to the oxidation of CO on the

terraces, step and kink sites [42-44]. However, in this case, a single peak is always observed (aside from the presence of occasional prewaves). The presence of multiple peaks is associated with a restricted mobility of CO on the surface, so that CO cannot move to the most catalytic sites, that is, the step and kink sites. This means that the mobility of CO is significantly different on the Pt(111) and the Pt(100) surfaces. In order to determine this, transient oxidation experiments were carried out on these surfaces (fig. 10). The obtained currents for the transients were fitted using the two typical kinetic models for the CO oxidation, the Langmuir-Hinselwood (L-H) mean field equation and the nucleation and growth model (not shown) [18, 45]. As can be seen in the figure, the L-H model is able to fit perfectly the transient. In order to fulfill this equation, the mobility of the CO molecules on the surface has to be fast, so that a random distribution of CO and OH adsorbed species is obtained at any time during the oxidation process.

A second difference with the other platinum single crystal electrodes is that the presence of prewaves is only observed for n<12 [42, 46], and was previously observed for the Pt(100) electrode[42, 44]. The differences may arise from the different coverages obtained in this work. As aforementioned, the conditions for CO adsorption are mild, and therefore, it is possible that we have not reached the maximum coverage. Since prewaves are normally associated with compressed adlayers [47-49], the use of mild adsorption conditions may avoid the formation of compressed adlayers, and therefore, lead to the absence of prewaves in the oxidation profile.

3.4. Spectroelectrochemical results

In order to make some molecular considerations on the CO oxidation on Pt(S)[n(100)×(111)] stepped surfaces in alkaline media some FTIR measurements were made. In the following spectra the positive bands correspond to the products formed at the sampling

potential, while negative bands arise due to the consumption of species present at the reference potential. The CO was adsorbed on the surface by bubbling CO gas in the cell atmosphere, with the surface in the solution at a controlled potential of 0.1V. This potential was maintained until the electrode was pressed against the CaF_2 window. From that value, the potential was stepped progressively and the different spectra were recorded.

In the obtained spectra (Figure 11), 3 main bands can be observed at 1994-2004, 1873 and 1397 cm^{-1} depending on the electrode potential. The band at 1397 cm^{-1} corresponds to carbonate formed from the oxidation of CO. At low potentials, just the bands at 1994-2004 and 1873 cm^{-1} are observed. The frequencies of these bands fit well with those for the stretching of CO molecules bonded on Pt(100) in on-top and bridge configuration, respectively [50]. As has been reported, the relative intensity of these two peaks in acidic solutions strongly depends on the coverage and electrode potential [50, 51]. For high coverages, on-top CO binding predominates (θ_{CO}~ 0.75) while for coverages lower than 0.25 the bridge CO is the dominant band. In all cases, the band intensity for the bridged CO diminishes as the potential is increased. The attenuation of bridging CO coordination on Pt(100) at more positive potentials has also been observed in STM measurements [52]. This interconversion phenomena reflects the stabilization of the CO bonded in bridge configuration at lower potentials through a back donation mechanism that is stronger in this geometry as reflected by its lower vibrational frequency [50].

This effect is also observed in alkaline media. Since the absolute potential is ca. 0.8 V more negative than in acidic solutions, the bridge CO band dominates on the spectra. Also, when the electrode potential is increased the intercoversion takes place and the on-top CO band intensity slightly increases. In principle, it could be possible to predict the frequencies of the CO bands in alkaline media using the spectra and the Stark tuning slope measured in acid media and viceversa. However, the frequency is not only dependent on the electrode potential

but also on the relative populations of both species. Thus, nonlinear changes in frequencies are observed for the bridge CO band when its intensity is low [50]. At potentials as low as 0.5 V, CO oxidation is already observed and at 0.7 V, the whole CO adlayer has been oxidized, as observed by the negative band at 1390 cm^{-1} characteristic of carbonates. A less intense band at 1614 cm^{-1} can also be observed corresponding to water bending. Incidentally, carbonate adsorption does not cause any modification of the CO stripping voltammetry, which takes place in a single peak.

For the different stepped surfaces, no qualitative changes are observed in the spectra with respect to that of the Pt(100) electrode (figure 12). In all cases, the bridge CO band dominates the spectra at 0.1 V with a very small contribution of on-top CO. Also, the band frequency for the bridge CO does not change significantly with the step density. This fact means that the electronic characteristics of the Pt-CO bond are not significantly affected by the presence of steps. It is also worth to note that there is no distinction between the bands corresponding to CO adsorbed on terrace and step sites. This is, however, expected since for very close vibrating dipoles it is well described that dipole coupling leads to an intensity transfer from the low frequency mode to the high frequency mode, resulting in the observation of a single vibrational band [53]. Only in the case of Pt(711) a splitting of the band corresponding to CO adsorbed on top can be observed.

4. Conclusions

The voltammetric behavior of these electrodes at different pH and charge displacement experiments allow the assignment of the different signals appearing in the voltammetry to different processes on terrace and step sites and to establish the nature of the species present on the surface at different potentials. At 0.2 V, the charge of the surface is compatible with a state in which OH is adsorbed on the step sites and blocks half terrace site and hydrogen is

adsorbed on the remaining terrace sites. At 0.7 V, the coverage of OH is ca. 0.5. From a qualitative point of view, the behavior of the surfaces can be divided into two groups: those with wide terraces, for which the differences with the Pt(100) surface are small, and the surfaces with narrow terraces, which had a very distinctive behavior. This scheme is also reproduced when the pztc of the surfaces is examined: for surfaces with wide terraces the changes of the pztc are very small, whereas for n<7, a significant diminution of the pztc is observed.

CO adsorption and oxidation on these surfaces has also been studied. In all cases, a single peak is observed (aside the presence of occasional prewaves). Chronoamperometric analysis of the transients is in agreement with the L-H mean field model, which implies that the mobility of CO on the surface is large. The presence of steps catalyzes the oxidation of CO, since the stripping peak shifts towards more negative potentials. Additionally the FTIR spectra revealed that the CO is mostly bonded in bridge configuration interconverting to on-top configuration when the electrode potential is increased.

Acknowledgements

The work was carried out under financial support by the European Commission (through FP7 Initial Training Network ‘‘ELCAT”, Grant Agreement No. 214936-2) and MICINN (project No. CTQ2010-16271).

References.

[1] A. Rodes, K. Elachi, M.A. Zamakhchari, J. Clavilier, J. Electroanal. Chem., 284 (1990) 245.

[2] A. Rodes, M.A. Zamakhchari, K. Elachi, J. Clavilier, J. Electroanal. Chem., 305 (1991) 115.

[3] J. Clavilier, J.M. Feliu, A. Fernández-Vega, A. Aldaz, J. Electroanal. Chem., 269 (1989) 175.

[4] J.M. Feliu, A. Rodes, J.M. Orts, J. Clavilier, Pol. J. Chem., 68 (1994) 1575.

[5] A. AlAkl, G.A. Attard, R. Price, B. Timothy, J. Electroanal. Chem., 467 (1999) 60.

[6] A. Al-Akl, G. Attard, R. Price, B. Timothy, Phys. Chem. Chem. Phys., 3 (2001) 3261.

[7] L.A. Kibler, A. Cuesta, M. Kleinert, D.M. Kolb, J. Electroanal. Chem., 484 (2000) 73.

[8] K. Domke, E. Herrero, A. Rodes, J.M. Feliu, J. Electroanal. Chem., 552 (2003) 115.

[9] N. Garcia-Araez, V. Climent, E. Herrero, J.M. Feliu, Surf. Sci., 560 (2004) 269.

[10] G.A. Attard, O. Hazzazi, P.B. Wells, V. Climent, E. Herrero, J.M. Feliu, J. Electroanal. Chem., 568 (2004) 329.

[11] F.J. Vidal-Iglesias, N. Garcia-Araez, V. Montiel, J.M. Feliu, A. Aldaz, Electrochem. Commun., 5 (2003) 22.

[12] T.J. Schmidt, P.N. Ross, N.M. Markovic, J. Phys. Chem. B, 105 (2001) 12082.

[13] N.M. Markovic, H.A. Gasteiger, N. Philip, J. Phys. Chem. B, 100 (1996) 6715.

[14] A. Rodes, V. Climent, J.M. Orts, J.M. Pérez, A. Aldaz, Electrochim. Acta, 44 (1998) 1077.

[15] F.J. Vidal-Iglesias, J. Solla-Gullón, V. Montiel, J.M. Feliu, A. Aldaz, J. Phys. Chem. B, 109 (2005) 12914.

[16] D.F. van der Vliet, M.T.M. Koper, Surf. Sci., 604 (2010) 1912.

[17] V. Climent, N. Garcia-Araez, E. Herrero, J. Feliu, Russ. J. Electrochem., 42 (2006) 1145.

[18] N.P. Lebedeva, M.T.M. Koper, J.M. Feliu, R.A. van Santen, J. Phys. Chem. B, 106 (2002) 12938.

[19] J. Clavilier, D. Armand, J. Electroanal. Chem., 199 (1986) 187.

[20] B. Lang, R.W. Joyner, G.A. Somorjai, Surf. Sci., 30 (1972) 454.

[21] E. Herrero, J.M. Orts, A. Aldaz, J.M. Feliu, Surf. Sci., 440 (1999) 259.

[22] J. Clavilier, R. Albalat, R. Gómez, J.M. Orts, J.M. Feliu, A. Aldaz, J. Electroanal. Chem., 330 (1992) 489.

[23] J. Clavilier, R. Albalat, R. Gómez, J.M. Orts, J.M. Feliu, J. Electroanal. Chem., 360 (1993) 325.

[24] E. Herrero, J.M. Feliu, A. Wieckowski, J. Clavilier, Surf. Sci., 325 (1995) 131.

[25] R. Gómez, J.M. Orts, B. Alvarez-Ruiz, J.M. Feliu, J. Phys. Chem. B, 108 (2004) 228.

[26] M.E. Gamboaaldeco, E. Herrero, P.S. Zelenay, A. Wieckowski, J. Electroanal. Chem., 348 (1993) 451.

[27] J.M. Feliu, K. Domke, J.M. Campina, N. Garcia-Arraez, E. Herrero, Abstr. Pap. Am. Chem. Soc., 225 (2003) 448.

[28] A. Rodes, E. Pastor, T. Iwasita, J. Electroanal. Chem., 377 (1994) 215.

[29] V. Climent, R. Gómez, J.M. Orts, A. Rodes, A. Aldaz, J.M. Feliu, in: A. Wieckowski (Ed.) Interfacial Electrochemistry, Marcel Dekker, Inc., New York, 1999, pp. 463.

[30] R. Gómez, V. Climent, J.M. Feliu, M.J. Weaver, J. Phys. Chem. B, 104 (2000) 597.

[31] V. Climent, R. Gómez, J.M. Feliu, Electrochim. Acta, 45 (1999) 629.

[32] A. Cuesta, Surf. Sci., 572 (2004) 11.

[33] V. Climent, R. Gómez, J.M. Orts, A. Aldaz, J.M. Feliu, The potential of zero total charge of single-crystal electrodes of platinum group metals, in, vol. 97-17, The Electrochemical Society, Inc., Pennington, NJ, 1997, pp. 222.

[34] V. Grozovski, V. Climent, E. Herrero, J.M. Feliu, ChemPhysChem, 10 (2009) 1922.

[35] V. Grozovski, V. Climent, E. Herrero, J.M. Feliu, Phys. Chem. Chem. Phys., 12 (2010) 8822.

[36] V. Grozovski, V. Climent, E. Herrero, J.M. Feliu, J. Electroanal. Chem., In Press, Corrected Proof.

[37] A. Berna, V. Climent, J.M. Feliu, Electrochem. Commun., 9 (2007) 2789.

[38] A. Bjorling, E. Ahlberg, J.M. Feliu, Electrochem. Commun., 12 (2010) 359.

[39] J.M. Feliu, J.M. Orts, A. Fernández-Vega, A. Aldaz, J. Clavilier, J. Electroanal. Chem., 296 (1990) 191.

[40] N.P. Lebedeva, M.T.M. Koper, E. Herrero, J.M. Feliu, R.A. van Santen, J. Electroanal. Chem., 487 (2000) 37.

[41] C.A. Angelucci, E. Herrero, J.M. Feliu, J. Solid State Electrochem., 11 (2007) 1531.

[42] G. Garcia, M.T.M. Koper, Phys. Chem. Chem. Phys., 10 (2008) 3802.

[43] G. Garcia, M.T.M. Koper, Phys. Chem. Chem. Phys., 11 (2009) 11437.

[44] G. Garcia, M.T.M. Koper, J. Am. Chem. Soc., 131 (2009) 5384.
[45] M. Bergelin, E. Herrero, J.M. Feliu, M. Wasberg, J. Electroanal. Chem., 467 (1999) 74.
[46] R. Gisbert, G. García, M.T.M. Koper, Electrochim. Acta, 56 (2011) 2443.
[47] A. López-Cudero, Á. Cuesta, C. Gutiérrez, J. Electroanal. Chem., 586 (2006) 204.
[48] A. López-Cudero, A. Cuesta, C. Gutiérrez, J. Electroanal. Chem., 579 (2005) 1.
[49] A. Cuesta, A. Couto, A. Rincón, M.C. Pérez, A. López-Cudero, C. Gutiérrez, J. Electroanal. Chem., 586 (2006) 184.
[50] S.C. Chang, M.J. Weaver, Surf. Sci., 238 (1990) 142.
[51] S.C. Chang, M.J. Weaver, J. Phys. Chem., 94 (1990) 5095.
[52] C.M. Vitus, S.C. Chang, B.C. Schardt, M.J. Weaver, J. Phys. Chem., 95 (1991) 7559.
[53] I. Villegas, M.J. Weaver, J. Chem. Phys., 101 (1994) 1648.

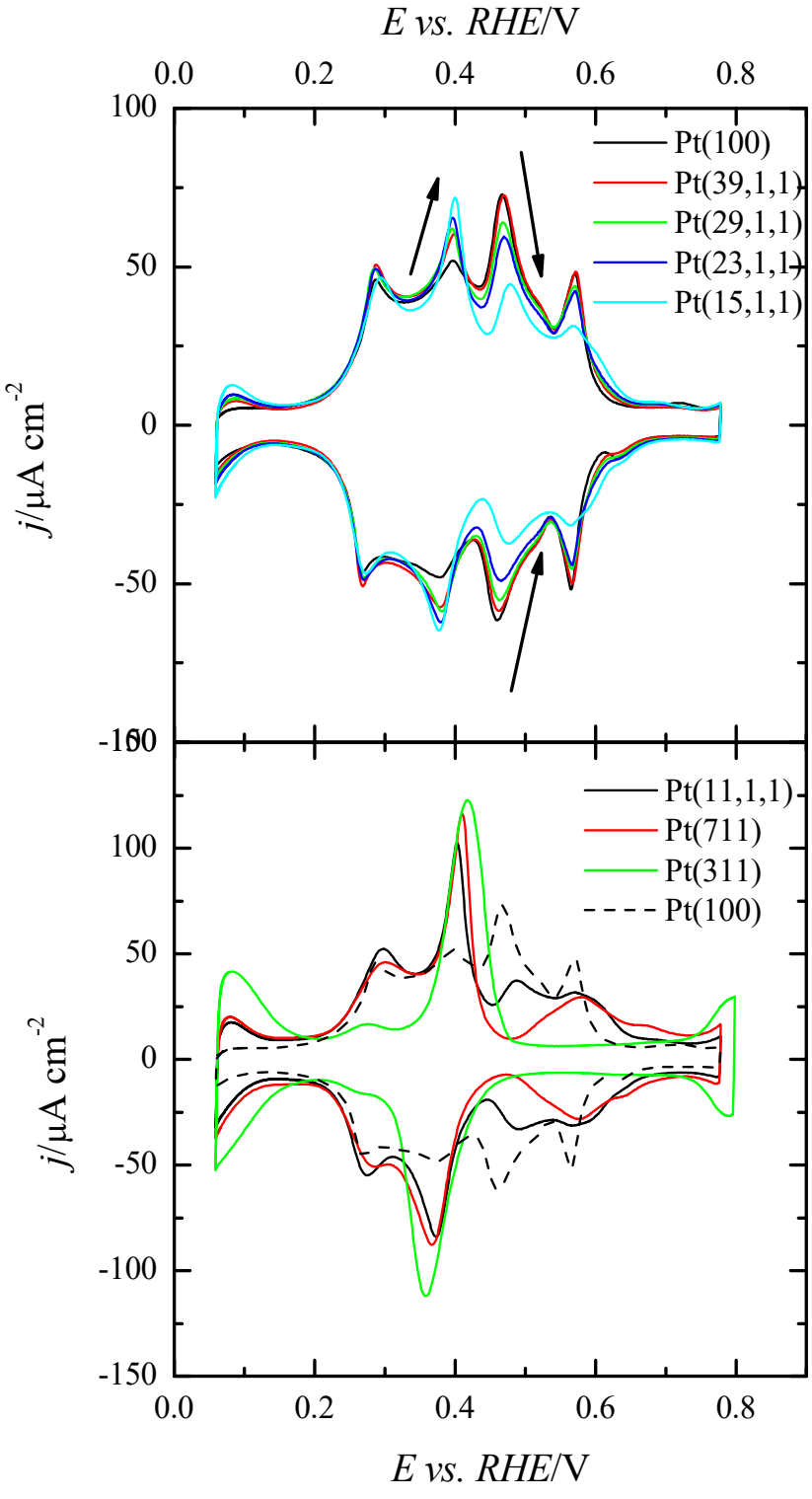

Figure 1. Voltammetric profile of Pt(S) [n(100)×(111)] surfaces in 0.1M NaOH. Scan rate: 50 mV s^{-1}. Arrows indicate changes with increasing step density.

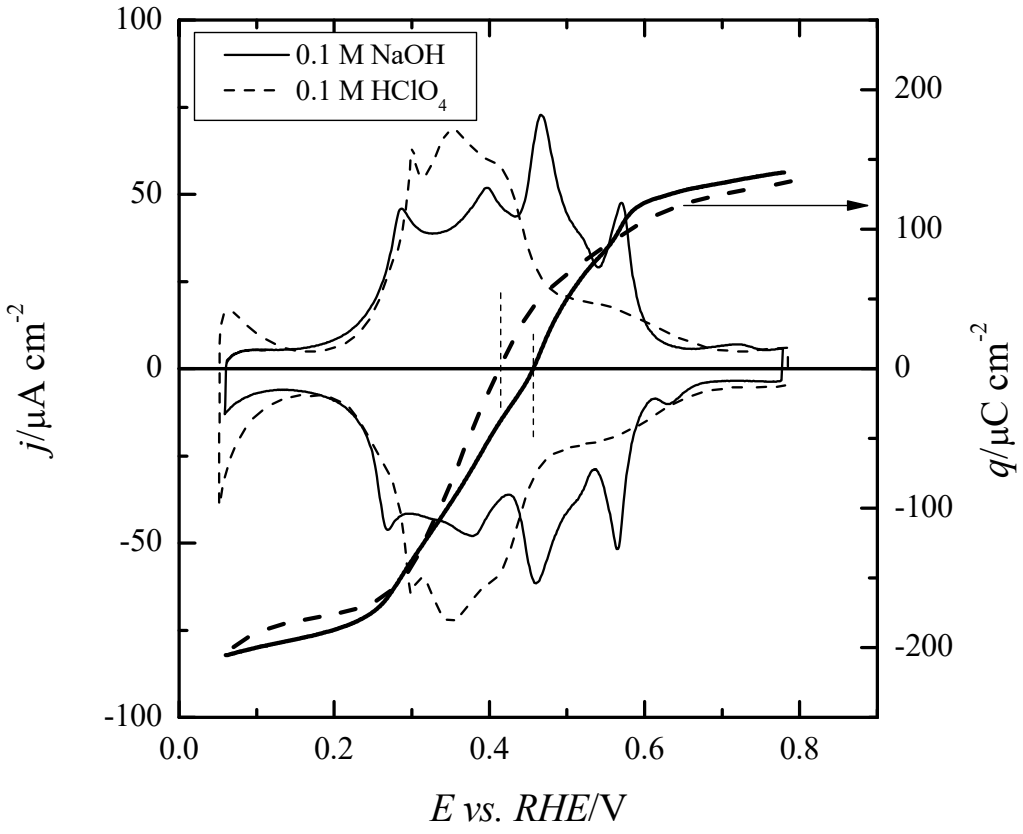

Figure 2. Voltammetric profile (left axis) and total charge density curves (right axis) for the Pt(100) electrode in 0.1M NaOH and 0.1 M $HClO_4$. Scan rate: 50 mV s^{-1}.

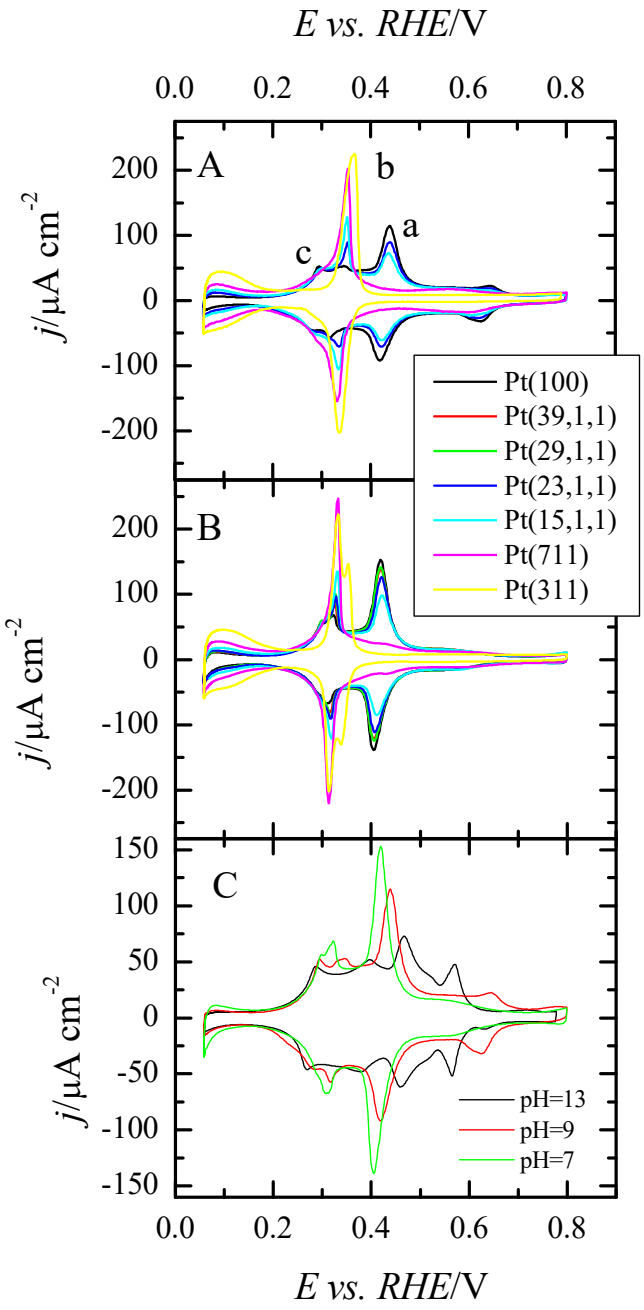

Figure 3. Voltammetric profile of Pt(S) [n(100)×(111)] surfaces in 0.1 M phosphate buffer pH=7 (A) and pH=9 (B). C) Comparison of the voltammogram of Pt(100) in the three different pHs as indicated. Scan rate 50 mV s^{-1}.

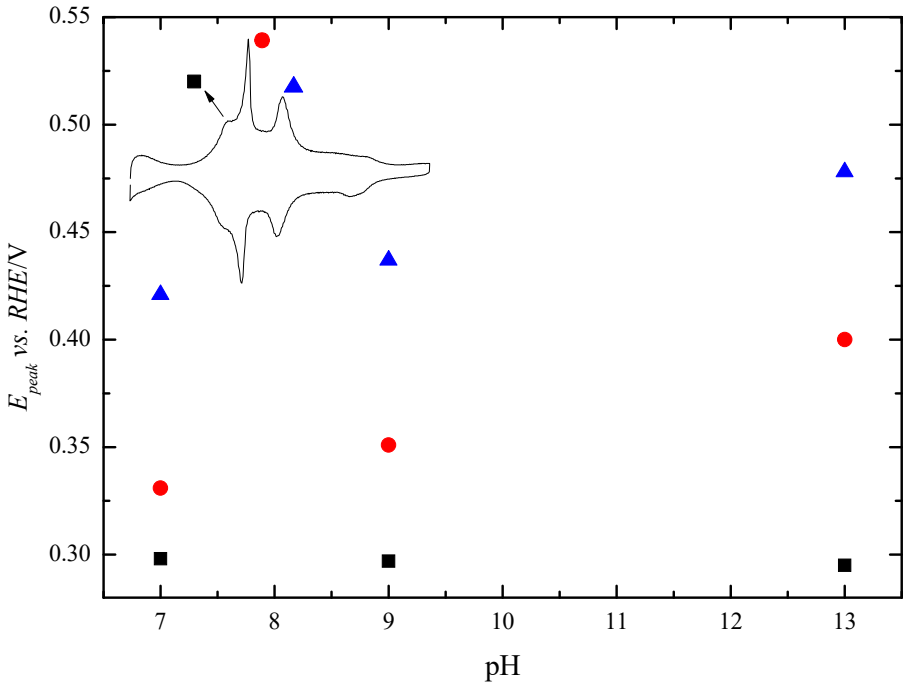

Figure 4. Peak potential from the voltammogram corresponding to the Pt(15,1,1) surface plotted as a function of the pH.

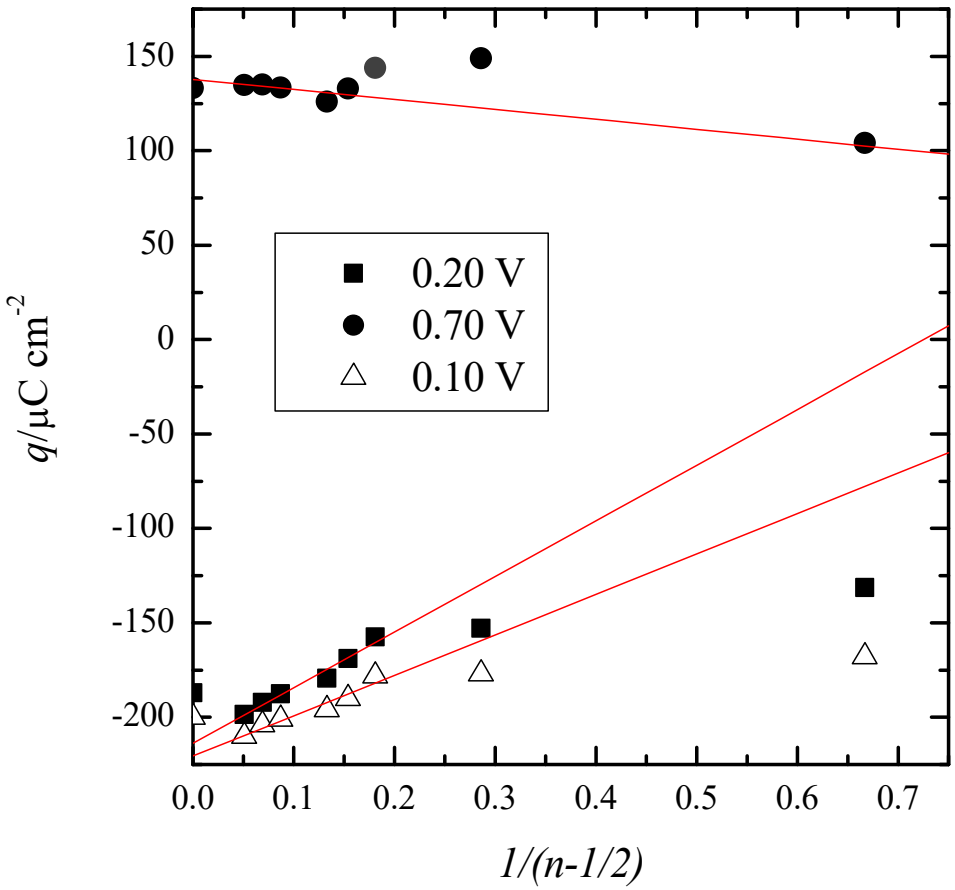

Figure 5. Total charge measured at 0.10 V, 0.20 V and 0.70 V in the voltammetry in 0.1 M NaOH using equation (4) vs. 1/(n-1/2) for the surfaces Pt(S)[n(100x(111)].

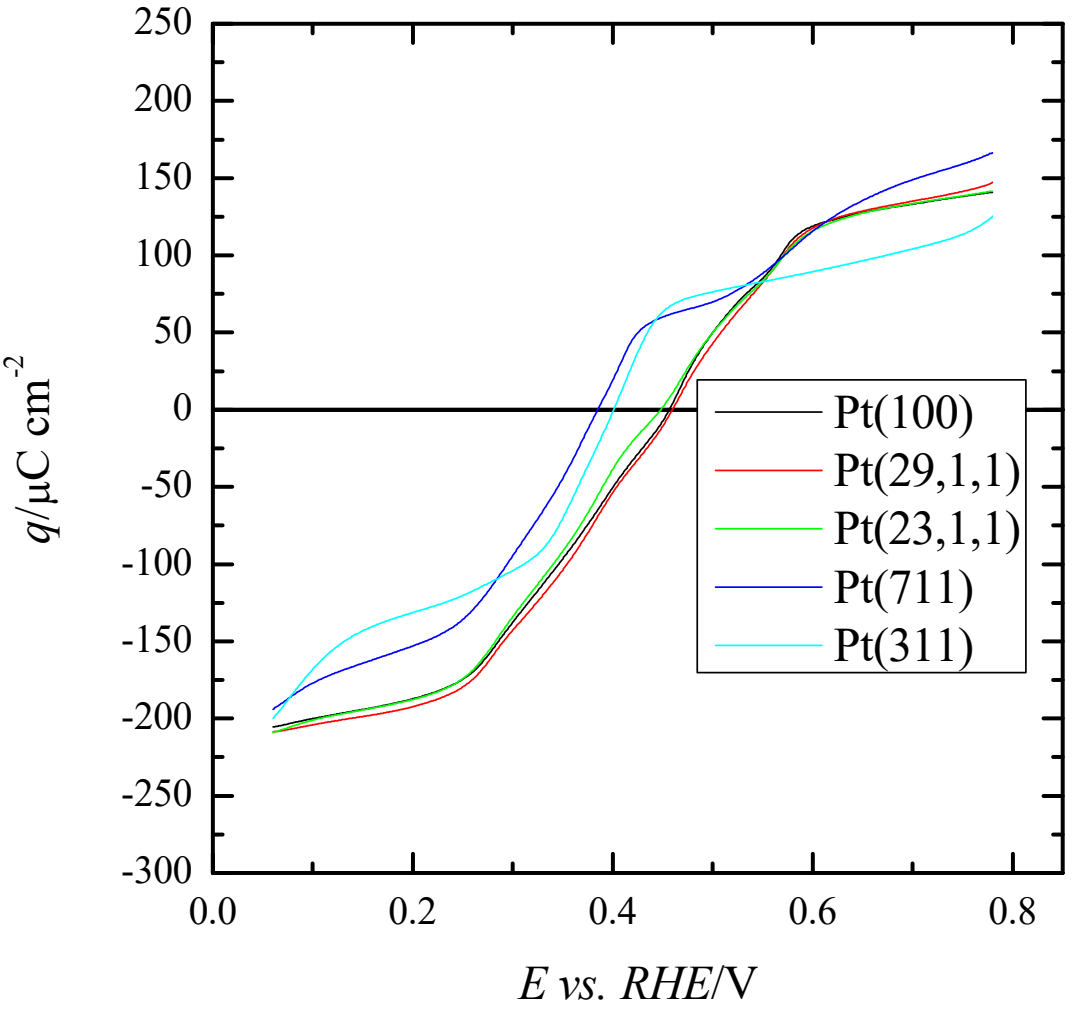

Figure 6. Total charge calculated according equation (3) vs. electrode potential for the surfaces under study in 0.1M NaOH.

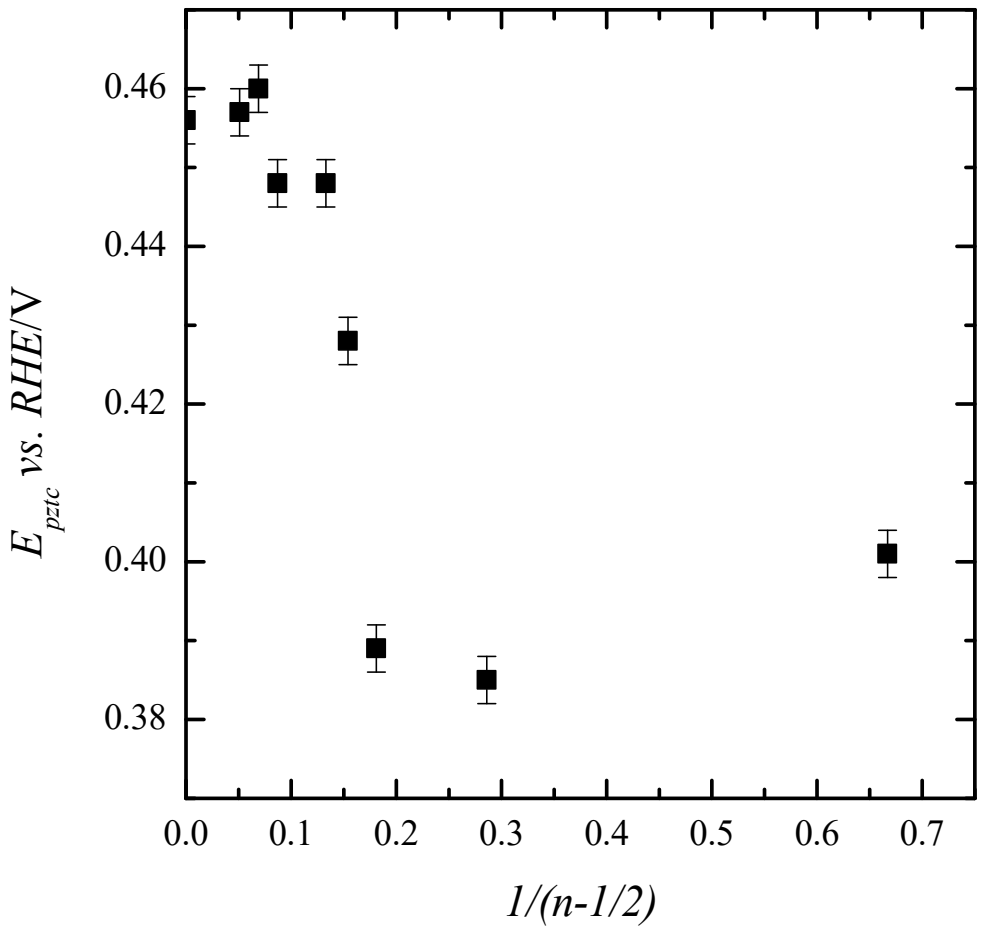

Figure 7. E_{pzet} vs. (1/(n-1/2)) in 0.1 M NaOH.

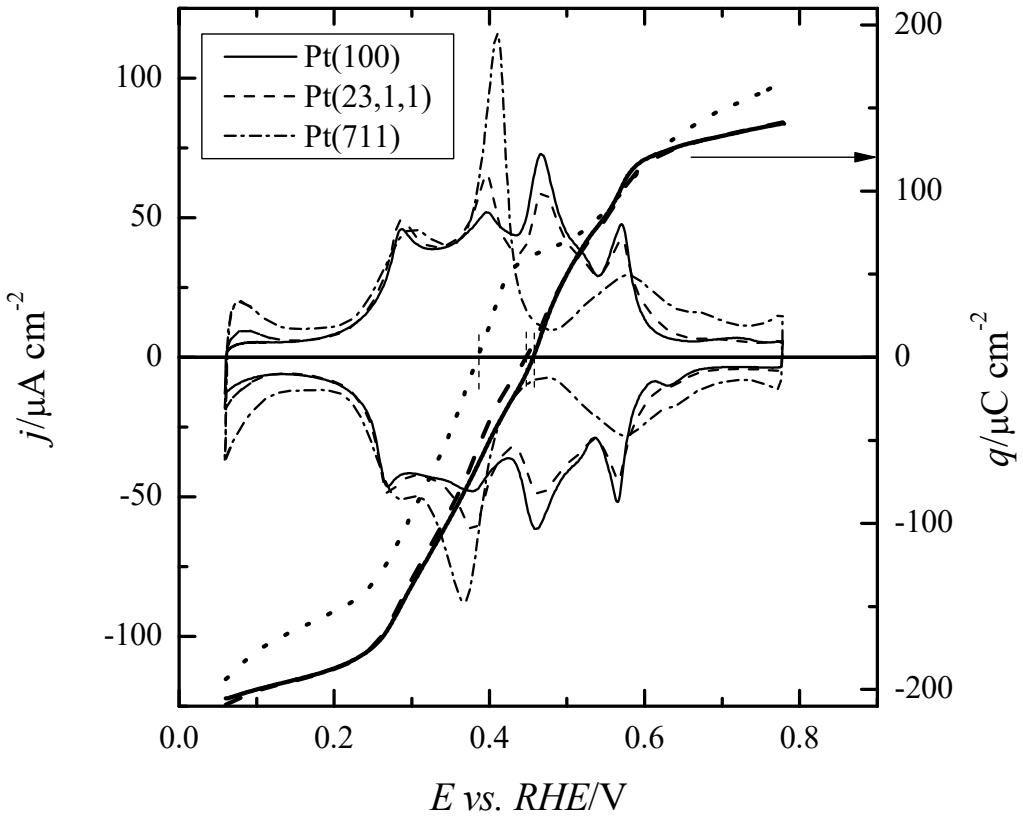

Figure 8. Voltammetric profile (left axis) and total charge density curves (right axis) for the Pt(100), Pt(23,1,1) and Pt(711) electrodes in 0.1M NaOH. Scan rate: 50 mV s^{-1}.

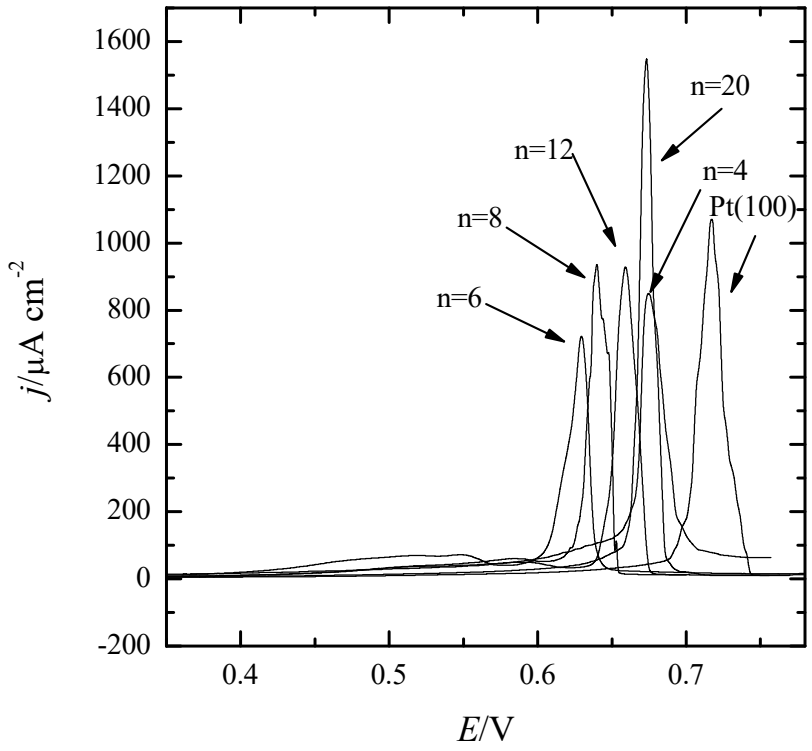

Figure 9. CO oxidation peaks obtained Pt(100) stepped surfaces with different number of terrace atoms in 0.1 M NaOH. Scan rate: 50mV s^{-1}.

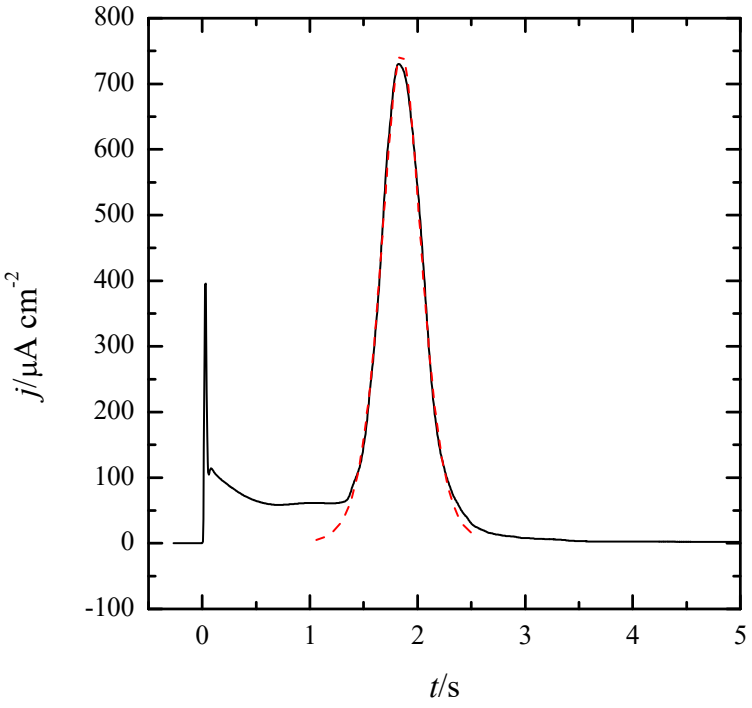

Figure 10. CO oxidation transient for the Pt(100) electrode measured at 0.65 V in 0.1 M NaOH. Dashed line: fitting with the Langmuir-Hinselwood mean field kinetics.

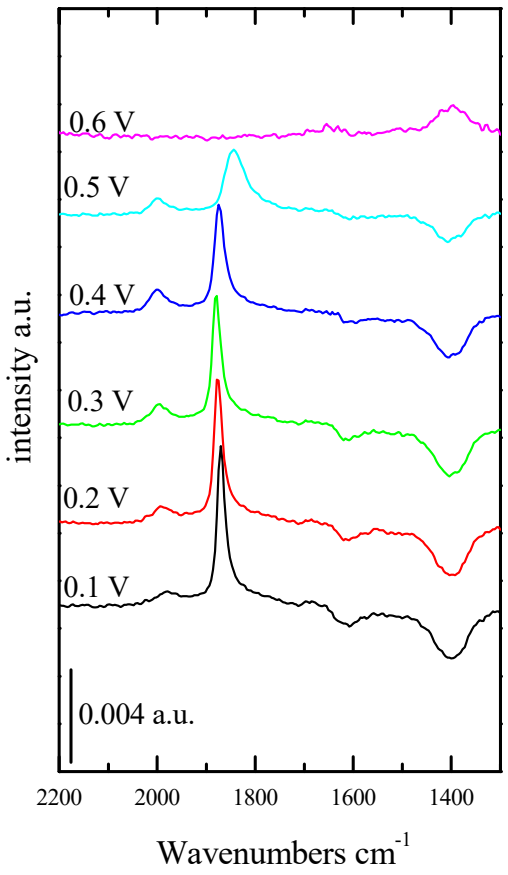

Figure 11. Spectra obtained for adsorbed CO on the Pt(100) electrode at different potentials, as labeled, in 0.1M NaOH. The reference spectra was taken at 0.1 V.

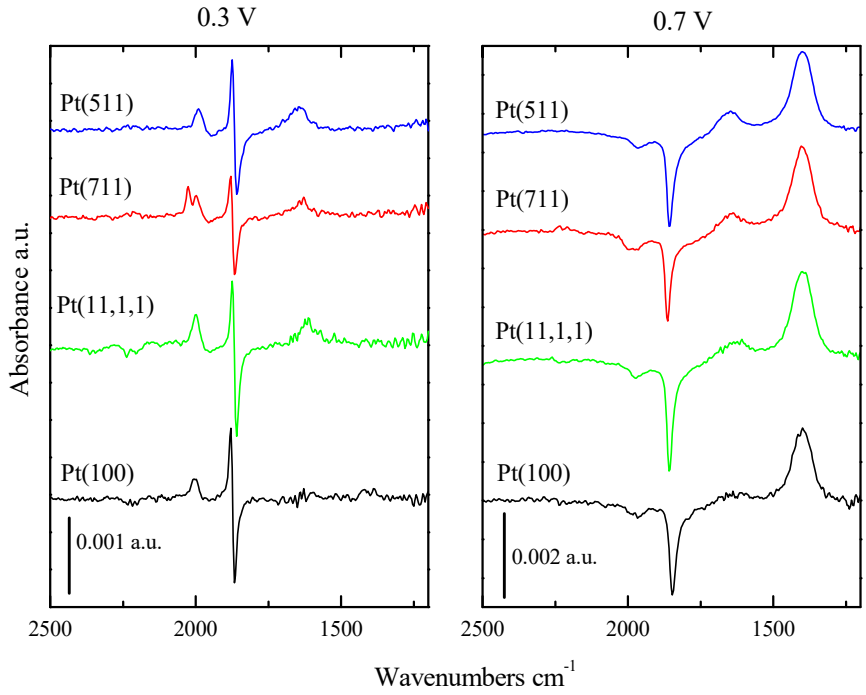

Figure 12. Spectra obtained for adsorbed CO on the Pt(100), Pt(11,1,1), Pt(711) and Pt(511) electrodes in 0.1M NaOH. Reference potential 0.1 V and sample potential: A) 0.3 and B) 0.7 V.